MR Imaging of the Acoustic Nerves and Small Acoustic Neuromas at 0.6 T: Prospective Study

Paul F. J. New, Terry B. Bachow, Gary L. Wismer, Bruce R. Rosen and Thomas J. Brady

AJNR Am J Neuroradiol 1985, 6 (2) 165-170
http://www.ajnr.org/content/6/2/165

MR Imaging of the Acoustic Nerves and Small Acoustic Neuromas at 0.6 T:

Prospective Study

Paul F. J. New[1]
Terry B. Bachow[1]
Gary L. Wismer[1]
Bruce R. Rosen[1]
Thomas J. Brady[2]

To evaluate the capability of magnetic resonance (MR) in imaging normal acoustic nerves, 12 volunteers without signs or symptoms of intracranial disease were examined using a 0.6 T superconductive system. Several spin-echo (SE) pulse sequences were tested to identify the optimal sequence for demonstration of the acoustic nerve bundle. Repetition times (TRs) varied from 300 to 2000 msec and echo times (TEs) from 30 to 120 msec. A single-slice technique was used with 5 and 8 mm sections, one or two data acquisitions per projection, and axial and coronal imaging. The normal acoustic nerves were demonstrated readily by MR in axial and/or coronal sections. The distal parts of the nerves and tumors were imaged best with SE 1500/60. The medial extremities of the seventh and eighth nerves tended to be obscured in this sequence by brightening the cerebrospinal fluid signal adjacent to the brainstem, but they were demonstrated clearly with 500 or 800 msec TR and 30 msec TE. Five patients were studied who had hearing loss and evidence of retrocochlear disease. In four patients, MR imaging demonstrated five acoustic nerve tumors ranging in size from purely intracanalicular to a 12 mm cisternal component. In the fifth case, no tumor was identified by MR imaging or gas computed tomographic (CT) cisternography. Contrast-enhanced CT using a Siemens Somatom DR 3 or GE CT/T 8800 scanner failed to provide convincing evidence of tumor in any case, while gas CT cisternography was positive in all five tumors. All five acoustic neuromas were identified readily using the SE sequences that proved optimal for demonstration of normal nerves. This experience revealed that MR imaging can demonstrate the eighth nerve complex well and reliably. Single-slice (5 or 8 mm) technique is adequate, but multislice without tissue gaps (used recently) is more efficient. Small, even intracanalicular, acoustic neuromas are imaged effectively, indicating that the method is capable of superseding contrast CT cisternography, particularly with improving technology.

This article appears in the March/April 1985 issue of *AJNR* and the May 1985 issue of *AJR*.

Received August 30, 1984; accepted after revision October 22, 1984.

Presented in part at the annual meeting of the American Society of Neuroradiology, Boston, June 1984.

This work was supported by Public Health Service grant 1 KO4 CA 00848-03 awarded by the National Cancer Institute, Department of Health and Human Services.

[1] Department of Radiology, Massachusetts General Hospital, Boston, MA 02114. Address reprint requests to P. F. J. New.

[2] Medical Service, Massachusetts General Hospital, Boston, MA 02114.

***AJNR* 6:165–170, March/April 1985**
0195-6108/85/0602-0165

Currently, computed tomography (CT) with intravenous contrast enhancement is the preferred initial imaging technique when acoustic neuroma is suspected. This method usually demonstrates acoustic neuromas of 1.5–2 cm in diameter and, with high-resolution techniques, can reveal neuromas smaller than 1 cm [1, 2]. However, beam attenuation and interpetrous bone artifacts frequently cause false-negative or equivocal results if tumors are smaller than 1.5 cm. In the presence of neurosensory hearing loss, therefore, gas or water-soluble contrast CT cisternography is often required to establish or exclude the diagnosis [1–6]. Although readily learned, the techniques of CT cisternography are invasive, may cause the patient significant pain, and are subject to occasional technical failure or false-positive results [7–9]. There is also a very small but definite risk of significant morbidity and even mortality as the result of reaction to iodinated contrast medium given intravenously.

Magnetic resonance (MR) imaging is without identifiable biologic hazard at magnetic field strengths currently used, has inherently very high image contrast between neural structures and cerebrospinal fluid (CSF) when certain radiofrequency (RF) pulse sequences are used, and is free from bone artifacts [10–14].

For these reasons, we initiated a prospective study to test the capability of MR

TABLE 1: **Clinical Signs and Symptoms in Patients with Neurosensory Hearing Loss Studied with Magnetic Resonance Imaging**

Group 2 Case No.	Clinical Findings
1	R hearing loss; BSEP: retrocochlear disease; intracanalicular neuroma
2	Vertigo; sudden R hearing loss; BSEP: retrocochlear disease; neuroma protruding 4 mm from internal auditory canal
3	Neurofibromatosis; L hearing loss; tinnitus; abnormal BSEP; bilateral small neuromas, R > L
4	Neurofibromatosis; total L hearing loss; moderate R hearing loss; bilateral small neuromas; left previously excised
5	L tinnitus; bilateral hearing loss, L > R; audiometry: diminished discrimination on L indicated retrocochlear disease; clinical diagnosis: neuritis; no tumor

Note.—R = right; L = left; BSEP = brainstem auditory-evoked responses.

TABLE 2: **Angle of Acoustic Nerve Complex to Plane Used for MR Study of Normal Subjects**

Group 1 Case No.	Axial Angle			Coronal Angle		
	Right	Left	Difference	Right	Left	Difference
1	...	22	...	3	6	3
2	13	16	3	...	...	...
3	41*	29*	12	14	21	7
4	27	25	2	...	...	...
5	9*	13	4	...	...	...
6	25	15	10	...	...	...
7	8	9	1	...	...	...
8	32	32	0	...	...	...
9	0	0	0	3	5	3
10	5	17	12	10†	4†	6
11	13	3	10	...	...	...
12	...	5	...	...	...	...

Note.—Axial angle = angle of acoustic nerve complex to coronal plane as nerve passes through internal auditory canal and cistern; coronal angle = angle of nerve downward from horizontal plane. Ranges of angles: axial (0°–41°; differences, 0°–12°); coronal (3°–21°; differences, 3°–7°). Difference reflects right-left asymmetry.

* Slight anteromedial curve.

† Slight inferior convexity.

imaging in demonstrating the anatomy of normal acoustic nerve bundles and in detecting small acoustic neuromas. Observations were also made of deformity of the acoustic nerves caused by adjacent posterior fossa tumors.

Subjects and Methods

Twelve volunteers without evidence of neurologic disease were studied (group 1). Five patients with neurosensory hearing loss were studied also (group 2, table 1). Each of these patients had been examined with intravenous contrast-enhanced CT, with negative or equivocal results. Gas CT cisternography had also been performed in each case; in two of these patients, small masses consistent with acoustic neuroma had been demonstrated on one side (cases 1 and 2). In two cases of neurofibromatosis, gas CT cisternography had demonstrated bilateral tumors in one (case 3) and metrizamide CT cisternography had revealed bilateral tumors in the other (case 4). In case 4, the left-sided tumor had been excised 1 year before the MR study, and a recent gas CT cisternogram showed slight interval enlargement of the remaining tumor. In the fifth case in this group, gas CT cisternography was interpreted as indicating left auditory nerve atrophy. The patient had complained of bilateral deafness, worse on the left side, and a final diagnosis of bilateral eighth nerve neuritis was made.

Two other patients, one with a posterior fossa and craniobasal chondrosarcoma grade I and one with an inferior lateral cerebellar hemispheric tumor, were also studied with CT and MR, and were added to this report because interesting acoustic nerve distortions were observed on MR only. All of the CT examinations were performed using a Siemens Somatom DR3 or GE CT/T 8800 or 9800 scanner. Intravenous contrast enhancement was performed with a drip infusion of 300 ml of Urovist and sections were 4 and 5 mm in thickness, contiguous or overlapped. For CT cisternography, 1.5 or 2 mm contiguous sections were obtained.

The MR studies were approved by the Massachusetts General Hospital Subcommittee for Human Studies, and informed consent was obtained from all subjects. All of the MR studies were performed with a 0.6 T superconductive magnet system (Teslacon, Technicare Corp., Solon, OH), operating at a proton resonance frequency of 25.4 MHz. In all subjects, except case 4 of group 2, sequential 2-D single-slice techniques were used. Nominal pixel size was 2.0 × 1.0 mm (x axis matrix, 256; y axis [phase encoding gradient], 128, interpolated to 256). A slice thickness of 8 mm was used in all group 1 subjects but one, in whom 5 mm sections were obtained. In case 4, multislice imaging with 7.5 mm sections was used, without apparent tissue gaps, following upgrading of software. Both axial and coronal planes were used to study all patients, but coronal imaging was not always used in group 1 subjects (table 2).

Spin-echo (SE) sequences with repetition times (TRs) of 300, 500, 1000, 1500, and 2000 msec were used with echo delays (TEs) of 30, 60, and 120 msec. The various SE sequences were combined in different ways in different subjects to determine the most suitable combination of parameters. In one subject in group 1, an inversion-recovery (IR) sequence was used with a 1500 msec TR, 450 msec inversion time (TI), and 180° refocusing pulses (30 msec TE). One or two readings were obtained per projection. Acquisition times were 2.2 min for 500 msec TR and 4.5 min for 2000 msec TR (for single or multislice technique); they were twice as long with two readings per projection.

The anatomy of the normal eighth nerve bundles was examined to provide a basis for evaluation of imaging technique and the pathologic anatomy in patients with acoustic neuromas and lesions adjacent to the seventh and eighth nerve complex.

Results

In all 12 cases in group 1, one or both acoustic nerve complexes were demonstrated. If, due to asymmetric anatomy and/or patient positioning, only one acoustic nerve was demonstrated in axial section, no attempt was made to localize and study the other nerve. Combining the axial and coronal sections, 23 of the 24 nerves were demonstrated (fig. 1). The inclinations of the auditory nerves relative to the coronal plane in axial images and to the horizontal plane in coronal sections were measured, and asymmetries, if present, were noted (fig. 1A). In one individual, both acoustic nerves lay in the coronal plane. In 11, the nerves inclined anteriorly between the brainstem and the lateral extremity of the internal auditory canal (IAC), usually asymmetrically. A slight anteromedial convexity of the cisternal part of the nerve was demonstrated in three

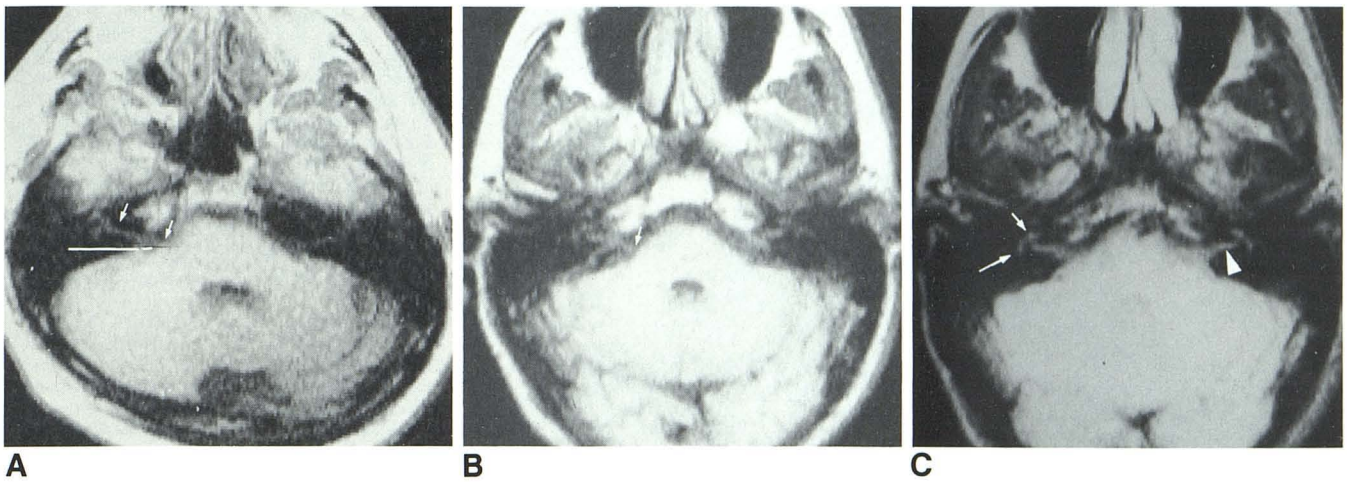

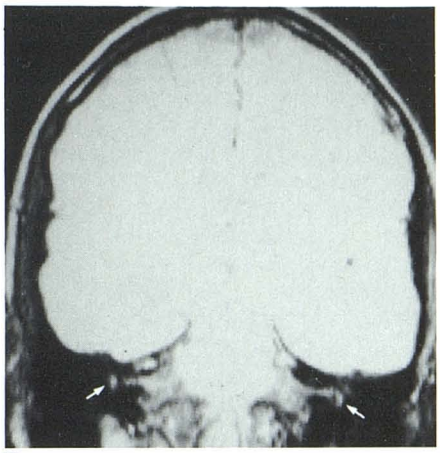

Fig. 1.—Eighth nerve complex in normal subjects. **A**, Axial SE 1000/30 of image right eighth nerve, 5 mm section, two readings/projection. Nerve complex is visible through IAC to brainstem (*arrows*). Angle between eighth nerve and coronal plane is indicated by *white line*. **B**, Axial SE 500/30 image, two readings/projection, 8 mm section. Medial extremity of nerve complex can be traced to brainstem (*arrow*). S/N ratio is lower than when msec TR is used, owing to lesser remagnetization. **C**, SE 1500/60 image, same subject as in **B**, one reading/projection, 8 mm thickness. Nerve complex within IAC is more clearly visible, as are cochlea (*short arrow*) and vestibule (*long arrow*). However, there is now increased signal from cisternal CSF, which obscures medial extremity of nerve complex. Left nerve, very poorly shown in **B**, is now well imaged within IAC (*arrowhead*). **D**, Coronal SE 1500/60 image, 8 mm thick, one reading/projection. Normal nerve complex is seen within IAC on each side. Part of cochlea (*arrows*). Cisternal parts of nerve largely obscured within relatively high signal of cisternal CSF with this sequence.

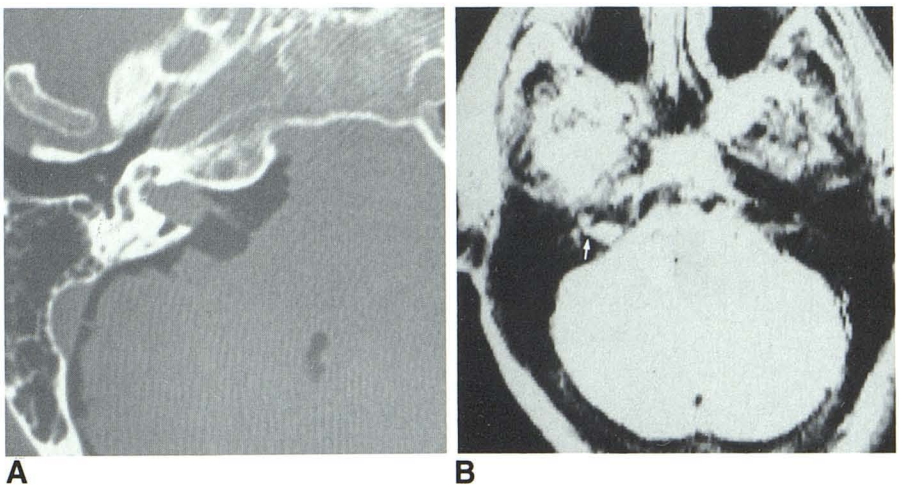

Fig. 2.—Case 2. **A**, Air CT cisternogram. Purely intracanalicular neuroma within moderately expanded IAC. Cisternal part of eighth nerve complex is not widened. **B**, Axial SE 1500/60 image, 8 mm section, one reading/projection. Neuroma seen clearly in IAC. Cisternal part of nerve complex obscured by bright cisternal CSF signal. Cochlea anterolaterally and vestibule posterolaterally are visible and neuroma extends to region of lamina cribrosa (*arrow*).

nerves in two subjects. The eighth nerves in four subjects, imaged in the coronal plane, showed asymmetric inclination caudad from the brainstem through the IAC (table 2).

In the four cases in group 2 shown to have a total of five small acoustic neuromas by CT cisternography, the smallest tumor was purely intracanalicular and the largest projected 12 mm into the cerebellopontine angle cistern. All of the tumors were demonstrated by MR (figs. 2–4). In case 5, no

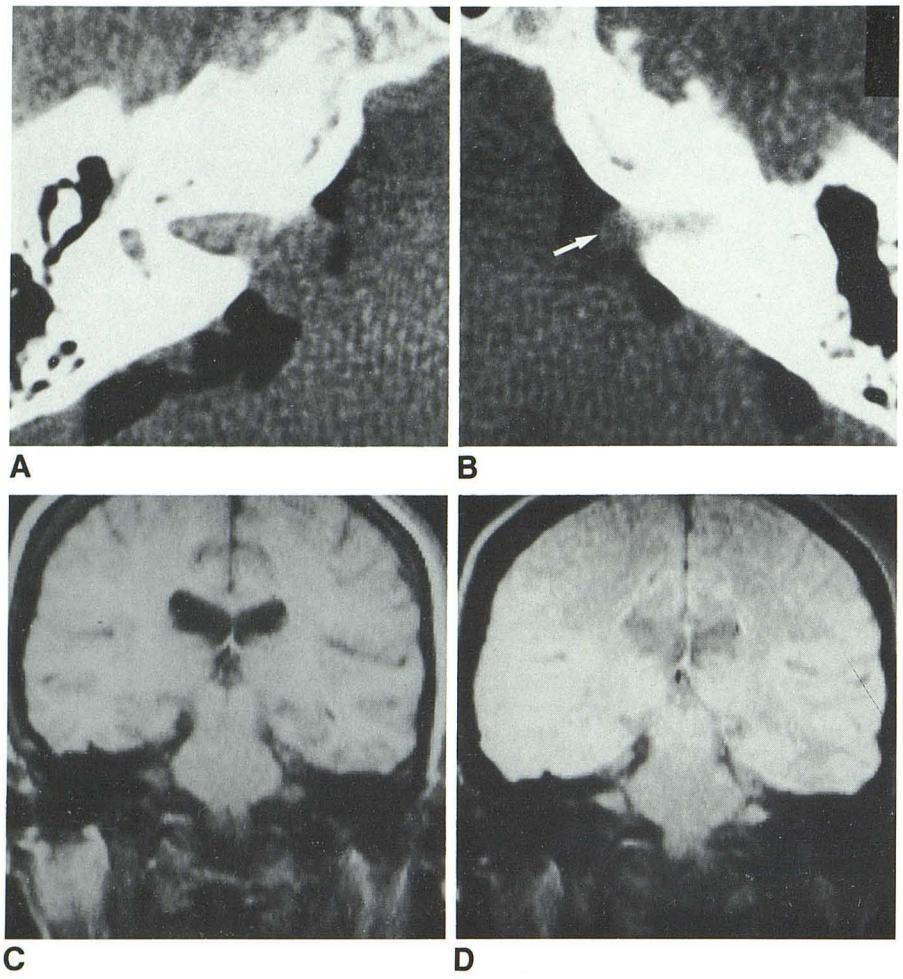

Fig. 3.—Case 3. Right (**A**) and left (**B**) gas CT cisternograms. Right neuroma protruding about 12 mm from mildly enlarged IAC and smaller neuroma projecting about 5 mm into left cistern (*arrow*). Coronal SE 500/30 (**C**) and SE 1500/60 (**D**) images, 8 mm sections, each with one reading/projection. Both tumors seen readily on both sequences, with brighter signal in **D**. No appreciable signal inversion of CSF in cerebellopontine angle cisterns in **D**, although patchy signal inversion is visible in lateral ventricular CSF. Right neuroma, which was found to taper into acoustic canal, was resected.

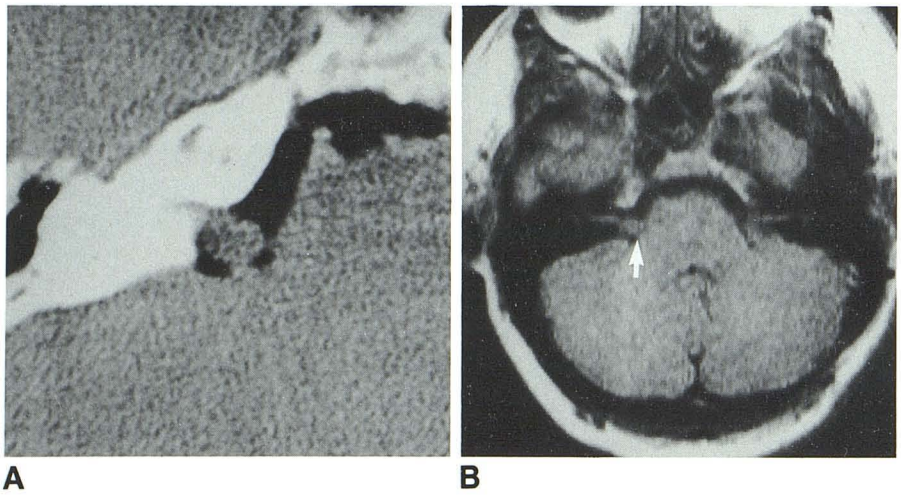

Fig. 4.—Case 4. Metrizamide CT cisternography had been performed 1 year before, demonstrating bilateral acoustic neuromas. Larger left-sided tumor was excised. **A**, Right-side gas CT cisternogram soon after MR. Little interval enlargement of neuroma, which measured about 8 mm in diameter and lay in cistern adjacent to normal-sized IAC. **B**, Axial SE 1000/30 image, 8 mm section, two readings/projection. Cisternal location of small tumor was demonstrated quite clearly, extending to surface of brainstem (*arrow*) (separation of medial surface of tumor from brainstem in **A** is explained by left lateral decubitus position in presence of cisternal air). Tumor does not appear to extend into IAC, where nerve appears normal. CSF has very little signal in this pulse sequence, allowing clear differentiation of tumor adjacent to brainstem. Signal of tumor is slightly less than of brainstem, which may result from volume averaging of adjacent CSF in 8 mm section. Total hearing loss had persisted in left ear. Left eighth nerve complex appeared slightly attenuated, but otherwise normal.

abnormality of morphology or signal intensity of the acoustic nerve was identified. Review of the CT cisternogram indicated that the appearance of atrophy of the nerve was due to a partial-volume effect.

As anticipated, IR resulted in poor contrast between the acoustic nerve complex and CSF and was used in only one subject. With our imaging system, the pulse sequence that produced the clearest definition of the acoustic nerves was

Fig. 5.—Normal subject. Axial SE 2000/90 image, 8 mm section, two readings/projection. Image is rather noisy due to long TE. CSF signal in entire fourth ventricle, cerebellopontine angle cisterns, and right IAC is bright relative to neural tissues, due to combination of long TR and long TE. Left IAC not included due to canting of head. With 8 mm section, lower intensity of acoustic nerve complex is not clearly identified within bright CSF in IAC or in cistern, due to volume-averaging. Under these circumstances, false-positive diagnosis of tumor in IAC or false-negative diagnosis with very small tumor in cistern is possible. With good S/N levels, thin sections would reduce possibility of diagnostic error.

Fig. 6.—Basal low-grade chondrosarcoma, markedly indenting pons (*arrowheads*). Axial SE 1500/60 image, 8 mm thick. Distortion of medial extremity of right acoustic nerve complex (*arrow*) causes nerve to incline posteriorly into and through IAC, a course found in no normal subjects (windowing for acoustic nerve). Normal hearing.

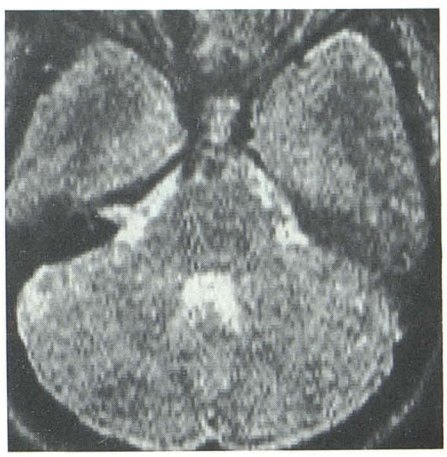

5

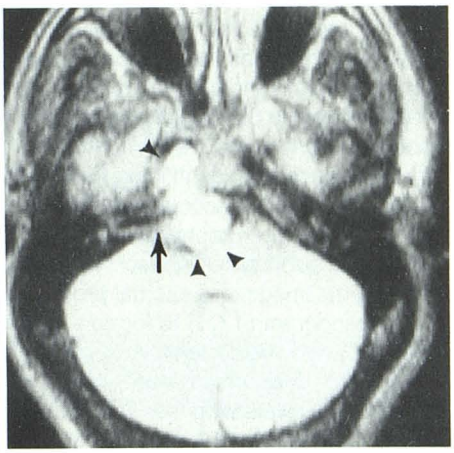

6

SE 1500/60. Both one and two readings per projection proved satisfactory. Accurate placement of 5 mm sections was more difficult than of 8 mm sections, was only used in one subject (from group 1), and required doubling of readings per projection or of TR (from 500 to 1000 msec) for similar signal-to-noise (S/N) ratios. Either method doubled the imaging time.

Because there was no evidence of significant partial-volume artifacts within the IAC with the chosen pulse sequence SE 1500/60, 8 mm sections were used routinely in groups 1 and 2. However, because this sequence tended to produce a signal intensity of CSF in the cerebellopontine angle cistern similar to that of neural tissues, the medial extremities of the seventh and eighth nerves tended to be obscured (fig. 1C). While acoustic neuroma seldom involves only the medial extremity of the eighth nerve, for clearest depiction of this part of the nerve bundle, an SE pulse sequence of shorter TR and TE is recommended in addition to SE 1500/60. TRs of 500 or 1000 msec and 30 msec TEs were found suitable for this purpose (figs. 1A, 1B, and 4B). More T2-weighted sequences, which produce intense CSF signal, obscure the nerve bundle in 8 mm sections (fig. 5).

The accuracy of MR was equal to that of CT cisternography in detecting the acoustic neuromas and highly superior to intravenous contrast-enhanced CT in demonstrating distortion of the acoustic nerves in the two patients with regional mass lesions (fig. 6).

Discussion

Our small prospective study provides evidence that MR has the potential to be the imaging method of choice for the diagnosis of acoustic neuromas, particularly acoustic neuromas smaller than 1.5 cm in diameter, demonstration of which is unreliable using CT with intravenous contrast enhancement. Although the spatial resolution of thin-section CT cisternography is superior, allowing resolution of the seventh and eighth nerves separately, it has been demonstrated that relatively thick MR sections (8 mm) are capable of providing satisfactory resolution of the eighth nerve complex within the IAC and of intracanalicular tumor. This is because the compact bone and air cells of the petrous pyramid contribute negligible signal, and the CSF, with its very long T1, provides a low-signal-intensity background on T1-weighted and moderately T2-weighted images, against which the seventh and eighth nerve bundles stand out in contrast. With the imaging system used in our study, the intensity of CSF in the IAC remains low with SE 1500/60. With this TR, a TE of 60 msec produced partial conversion of the fourth ventricular CSF to isointensity with brain substance (fig. 1C). SE 2000/90 produced increased signal intensity of fourth ventricular, cerebellopontine cisternal, and IAC CSF relative to brain (fig. 5). Under these circumstances, partial-volume effects of nerve or small neuroma and surrounding CSF become significant. Also, there is then risk of a false-positive diagnosis of acoustic neuroma. Here, thinner sections, as obtained by Daniels et al. [15], using 1.4 and 1.5 T systems, would have an advantage, but would require proportionately increased signal averaging (readings/projection) to maintain the S/N ratio compared with thicker sections. At 0.6 T, imaging time would be unduly prolonged with 3 mm single sections. A further disadvantage of very thin sections is indicated by the anatomic orientation of the eighth nerve bundles in axial and coronal planes. The nerves generally show an anterior course from brainstem in the axial plane and a downward inclination in the coronal plane. These configurations indicate that often it would be necessary to use several thin sections (e.g., 3 or 4 mm) in both imaging planes to record the complete course of the nerve. In multislice imaging with gaps between the imaged sections, a second multislice sequence with an appropriate change in location of the slice-selective RF pulses would be required to avoid skip areas, and the full course of a nerve would only be traced on multiple sections.

Whether 8 mm or thinner sections are used, the SE pulse sequences should be chosen so that CSF in the cistern and IAC exhibits a low-intensity signal. Because the signal from the normal nerve, and presumably from acoustic neuroma, increases as TR is increased from 500 to 1500 msec and TE from 30 to 60 msec, SE 1500/60 (for the IAC region) and SE 500/30 or SE 1000/30 (for the cisternal region) pulse se-

quences appeared optimal on our system. Somewhat different pulse sequences might prove to be optimal using other imaging systems and different static magnetic field strengths.

With the above SE sequences, the relatively rapidly flowing blood in arteries and veins contiguous with the acoustic nerves produced no identifiable signal. The occasional false-positive diagnosis of acoustic neuroma caused by a vascular loop on CT cisternography [7] is therefore avoided.

Using the single-slice 2-D technique, it is appropriate to use a midsagittal image or a sagittal projection image (analogous to the scanogram of CT) to localize the level of the acoustic nerves. With multislice technique, accurate preliminary localization of the level of the acoustic nerves is less important. We are now evaluating the following additional MR techniques: the use of 256 projections in both *x* and *y* axes, increased signal averaging, with multislice technique without gaps between sections, and thin-section volume imaging. Gapless multislice (7.5 mm) imaging has markedly reduced the imaging time for acoustic nerve evaluation (now less than 30 min) for axial and coronal imaging. Increasing the *y* axis projections to 256 appreciably improves the spatial resolution in this axis, but at the expense of doubling imaging times with a given pulse sequence and number of averages. Thin-section and isotropic volume imaging provides 1.5 mm slice thickness, but for an SE 1250/60 sequence, requires 101 min for data accumulation.

ACKNOWLEDGMENTS

We thank Paul A. Beaulieu for technical assistance, Denise M. Tager for preparation of illustrations, and Edith Bell for manuscript preparation.

REFERENCES

1. Valavanis A, Dabir K, Hamdi R, Oguz M, Wellauer J. The current state of the radiological diagnosis of acoustic neuroma. *Neuroradiology* **1982**;23:7–13
2. Dubois PJ, Drayer BP, Bank WO, Deeb ZL, Rosenbaum AE. An evaluation of current diagnostic radiologic modalities in the investigation of acoustic neurilemmomas. *Radiology* **1978**; 126:173–179
3. Sortland O. Computed tomography combined with gas cisternography for the diagnosis of expanding lesions in the cerebellopontine angle. *Neuroradiology* **1979**;18:19–22
4. Kricheff II, Pinto RS, Bergeron RT, Cohen N. Air-CT-cisternography and canalography for small acoustic neuromas. *AJNR* **1980**;1:57–64
5. Grepe A, Greitz T, Noren G. Computer cisternography of extracerebral tumors using lumbar injection of water soluble contrast medium. *Acta Radiol [Suppl]* (Stockh) **1975**;346:51–62
6. Rosenbaum AE, Drayer BP, Dubois PJ, Black O. Visualization of small extracanalicular neurilemmomas by metrizamide cisternographic enhancement. *Arch Otolaryngol* **1978**;104:239–243
7. Johnson DW. Air cisternography of the cerebellopontine angle using high-resolution computed tomography. *Radiology* **1984**; 151:401–403
8. Khangure MS, Mojtahedi S. Air CT cisternography of anterior inferior cerebellar artery loop simulating an intracanalicular acoustic neuroma. *AJNR* **1983**;4:994–995
9. Solti-Bohman LG, Magaram DL, Lo WWM, et al. Gas-CT cisternography for detection of small acoustic nerve tumors. *Radiology* **1984**;150:403–407
10. Young IR, Burl M, Clarke GJ, et al. Magnetic resonance properties of hydrogen: imaging the posterior fossa. *AJNR* **1981**;2: 487–493, *AJR* **1981**;137:895–901
11. Bydder GM, Steiner RE, Young IR, et al. Clinical NMR imaging of the brain: 140 cases. *AJNR* **1982**;3:459–480, *AJR* **1982**;139:215–236
12. Bydder GM, Steiner RE, Thomas DJ, Marshall J, Gilderdale DJ, Young IR. Nuclear magnetic resonance imaging of the posterior fossa: 50 cases. *Clin Radiol* **1983**;34:173–188
13. Brant-Zawadzki M, Davis PL, Crooks LE, et al. NMR demonstration of cerebral abnormalities: comparison with CT. *AJNR* **1983**;4:117–124, *AJR* **1983**;140:847–854
14. McGinnis BD, Brady TJ, New PFJ, et al. Nuclear magnetic resonance (NMR) imaging of tumors in the posterior fossa. *J Comput Assist Tomogr* **1983**;7:575–584
15. Daniels DL, Herfkins R, Koehler PR, et al. Magnetic resonance imaging of the internal auditory canal. *Radiology* **1984**;151:105–108
16. Axel L. Surface coil magnetic resonance imaging. *J Comput Assist Tomogr* **1984**;8:381–384